Available on CMS information server CMS NOTE 20010/???

The Compact Muon Solenoid Experiment

Analysis Note

27 October 2010

Opposite sign di-lepton SUSY search at $\sqrt{s} = 7$ TeV

M. Edelhoff, L. Feld, N. Mohr, D. Sprenger

I. Physikalisches Institut B, RWTH Aachen University, Germany

Abstract

We present a search for Supersymmetry in opposite sign di-lepton final states using the data from 2010 proton-proton-running of the Large Hadron Collider. The final state signature consists of leptons, several hard jets and missing transverse energy. Since we observe good agreement of data to simulation and our background prediction methods, we conclude that there is no sign of flavour correlated di-lepton production accompanied by high jet activity and large missing transverse energy in the dataset of 34 pb^{-1}. We report an upper limit on the flavour correlated production of a new physics model within acceptance of our event selection.

Preliminary version

Contents

1 Disclaimer

Please note that most of the methods used in this analysis have also been documented in SUS-08-004, SUS-09-002 (AN-2009/83) and AN-2010/167.

2 Introduction

The standard model of particle physics (SM) leads to a number of unsolved issues like the hierarchy problem and it provides no solution for pressing questions arising from astrophysical observations, most notably dark matter. In Supersymmetry (SUSY) a natural candidate for dark matter can be found if R-parity conservation is assumed. Supersymmetric particles (sparticles) have not been observed up to now which implies that they have to be heavy. On the other hand to provide a solution to the hierarchy problem their masses have to be in the TeV range. These prejudices lead to a signature of (many) hard jets and large missing transverse energy.

The long anticipated and succesfull start of the Large Hadron Collider (LHC) with a center of mass energy of 7 TeV allows us to explore this new TeV range very early on. Of special interest are robust signatures in leptonic final states which can be probed with the CMS experiment. If R-parity is conserved the lightest neutralino escapes detection and no mass peaks can be observed in SUSY decay chains.

The purpose of this analysis is to observe or exclude a significant excess of di-leptons over the various backgrounds. The dataset consists of 34 $\mathrm{pb}^{-1}$of proton-proton collisions collected by CMS during LHC running in 2010.

In Sec. 3 we define the signal benchmark points, that are used in this analysis. Section 4 describes the technical details of the object selection and in Sec. 5 we discuss the measured lepton efficiencies. Section **??** describes the method used to determine the contribution of non-prompt leptons in the final event selection. In Sec. we define the signal region, which includes a discussion of the main expected standard model backgrounds and their yields. Here we also discuss the trigger and its efficiency. Section 7.1 deals with the background prediction method (opposite flavour subtraction), which is used to predict the number of top-pair events in the signal region. We also define a control region in data and test that the method holds. The results are presented in Sec. 8 and we discuss the main sources of systematic uncertaintes in Sec. 9. Finally we set a limit and conclude.

3 Signal

The CMS minimal supergravity low-mass benchmark points have been designed to cover different decay modes of the neutralinos within supersymmetry. The mass spectra of the benchmark points have been calculated using the Softsusy code [1]. All branching ratios have been calculated with the SUSYHit program [2] and the events are simulated using Pythia [3]. The k-factor for the cross section at 7 TeV is calculated using a modified version of Prospino 2 [4]. In mSUGRA observable signal is produced strongly followed be (very) long decay chains leading to several hard jets (at least two). The escaping neutralino leads to missing transverse energy. This fact allows to define a search region to observe an excess over the SM and is used as main event selection as described in Section 6. It consits of

- Two opposite sign same flavour leptons within acceptance of $p_T > 10$ GeV [1)] and $|\eta| < 2.4$.

[1)] In the first version of the note the lepton p_T cut was at 5 GeV, which gives a better sensitivity to low mass mSugra. The electrons are not fully commissioned to 5 GeV and since there was no excess observed, we took an conservative approach to raise the threshold for this year and to continue commissioning the electron identification at low p_T, such that we can use low p_T thresholds in the next year.

- High $H_T > 350\ GeV$ with at least to jets to be as model independent as possible.
- High $\not{E}_T > 150\ GeV$, which is set as such that we expect roughly one di-leptonic $t\bar{t}$ event in this years dataset.

The number of expected events in a given di-lepton channel varies with the mSUGRA point realised by nature. A range of benchmark points has been studied to anticipate different possible signal constellations and not tune towards a specific set of parameters. Figure **??** shows the fraction of di-leptonic events splitted by flavour for a di-lepton selection on generator level. In all studied benchmark points the flavour correlated production dominates over the uncorrelated production.

4 Physics objects

4.1 PAT workflow

From the AOD samples so called Pat-Tuples have been created using the following tags of the Physics Analysis Toolkit (PAT) in CMSSW_4_2_X.

```
cmsrel CMSSW_4_2_3
cd CMSSW_4_2_3/src
cmsenv
addpkg PhysicsTools/PatAlgos    V08-06-25
addpkg PhysicsTools/PatExamples V00-05-17

# deterministic calculation of FastJet corrections
addpkg RecoJets/Configuration                          V02-04-16
addpkg RecoJets/JetAlgorithms                          V04-01-00
addpkg RecoJets/JetProducers                           V05-05-03

addpkg MuonAnalysis/MuonAssociators                 V01-13-00
addpkg PhysicsTools/Configuration                        V00-10-14

addpkg RecoTauTag/RecoTau RecoTauDAVerticesPatch_V5
addpkg RecoTauTag/TauTagTools RecoTauDAVerticesPatch_V5
addpkg RecoTauTag/Configuration RecoTauDAVerticesPatch_V5

cvs co -d__temp__ -r1.1 UserCode/SuSyAachen/Configuration/python/pfTools.py
/bin/mv __temp__/pfTools.py PhysicsTools/PatAlgos/python/tools
rm -r __temp__


cvs co -rV00-04-48 -dSuSyAachen UserCode/SuSyAachen
```

All physics objects necessary for this analysis are included in the Pat-Tuples.

4.2 Datasets

We perform the analysis on events triggered by leptonic, hadronic and cross-object triggers and therefore use several primary datasets reconstructed in CMSSW_4_2_X. All datasets used are listed in Tab. 1.

We select only events that enter the officially produced good-run-list

```
/afs/cern.ch/cms/CAF/CMSCOMM/COMM_DQM/certification/Collisions11/7TeV/Reprocessing/
Cert_160404-163869_7TeV_May10ReReco_Collisions11_JSON.txt
```

and the total integrated luminosity amounts to

$$\mathcal{L}_{int} = (204 \pm 8)\ \mathrm{pb}^{-1}. \tag{1}$$

Table 1: Datasets used in this analysis.

DBS datasetpath
/DoubleElectron/Run2011A-May10ReReco-v1/AOD
/DoubleElectron/Run2011A-PromptReco-v4/AOD
/DoubleMu/Run2011A-May10ReReco-v1/AOD
/DoubleMu/Run2011A-PromptReco-v4/AOD
/MuEG/Run2011A-May10ReReco-v1/AOD
/MuEG/Run2011A-PromptReco-v4/AOD
/ElectronHad/Run2011A-May10ReReco-v1/AOD
/ElectronHad/Run2011A-PromptReco-v4/AOD
/MuHad/Run2011A-May10ReReco-v1/AOD
/MuHad/Run2011A-PromptReco-v4/AOD
/HT/Run2011A-May10ReReco-v1/AOD
/HT/Run2011A-PromptReco-v4/AOD

4.3 Simulated datasets

All simulated samples from CMSSW_4_2_X are listed in Tab 2. Please note that for the final version the proper Madgraph samples will be used (as soon as they are available).

Table 2: Used CMSSW datasets from 4_2_X.

DBS datasetpath	No. events	σ_{LO} [pb]	Name
/LMX_SUSY_sftsht_7TeV-pythia6/Fall10-START38_V12-v1/AODSIM	200000	varies	SUSY LMX
/TTJets_TuneZ2_7TeV-madgraph-tauola/Fall10-START38_V12-v2/AODSIM	1443404	90	tt+jets
/DYJetsToLL_TuneZ2_M-50_7TeV-madgraph-tauola/Fall10-START38_V12-v2/AODSIM	1084921	2350	Z+jets
/WToENu_TuneZ2_7TeV-pythia6/Fall10-START38_V12-v1/AODSIM	189069	8057	W+jets
/WToMuNu_TuneZ2_7TeV-pythia6/Fall10-START38_V12-v1/AODSIM	189069	8057	W+jets
/WToTauNu_TuneZ2_7TeV-pythia6/Fall10-START38_V12-v1/AODSIM	189069	8057	W+jets
/QCD_TuneD6T_HT-100To250_7TeV-madgraph/Fall10-START38_V12-v1/AODSIM	10842371	7000000	QCD
/QCD_TuneD6T_HT-250To500_7TeV-madgraph/Fall10-START38_V12-v1/AODSIM	4873036	171000	QCD
/QCD_TuneD6T_HT-500To1000_7TeV-madgraph/Fall10-START38_V12-v1/AODSIM	4034762	520	QCD
/QCD_TuneD6T_HT-1000ToInf_7TeV-madgraph/Fall10-START38_V12-v1/AODSIM	1541261	83	QCD

Each dataset is scaled to the desired luminosity if not illustrated differently. Additionally a k-factor has been applied for some of the datasets. The MC is reweighted to correct for the difference in the vertex multiplicity distribution as described in [25].

4.4 Common event selection

To select good collision events we require the event to contain a good primary vertex, which has to pass the following conditions

```
!isFake
ndof > 4
abs(z) <= 24
position.Rho <= 2.
```

4.5 Muons

The acceptance of the muons is restricted to $p_T > 5$ GeV and $|\eta| < 2.4$. Each muon has to be identified as a global muon and tracker muon. The track of the muon in the inner tracker has to have at least 11 hits and a χ^2/ndf of the global muon track below 10. The impact parameter of the muon track with respect to the position of the first deterministic annealing (DA) vertex is required to be below 200 μm in x-y and within 1 cm in z. Additionally we require the muons to be well measured by the request that the relative error from the track-fit is below 10%. The combined energy sum in cone of size dR = 0.3 around each muon has to be smaler than 15% of its energy. All cuts are summarised in Table 3.

Table 3: Overview of the muon selection.

Name	Pat memberfunction	Cut
p_T	pt()	$\geq 5.$
$\|\eta\|$	abs(eta())	≤ 2.4
GlobalPromptTight	muonID('GlobalMuonPromptTight')	
TrackerMuon	isTrackerMuon()	
Number of hits	track.numberOfValidHits	≥ 11
Good track fit	track.ptError()/track.pt()	≤ 0.1
Impact parameter	abs(dxy(pv))	≤ 0.02
Impact parameter	abs(dz(pv))	≤ 1
Isolation	(isolationR03().hadEt + isolationR03().emEt + isolationR03().sumPt) / pt	≤ 0.15

4.6 Electrons

The acceptance of the electrons is restricted to $p_T > 10$ GeV and $|\eta| < 2.5$. We restrict ourselves to the ECALs fiducial volume, thus exclude electrons within $1.4442 < \eta < 1.566$.

Additionally, a conversion rejection is performed requiring that the electron track has maximally one lost hit in the tracker. We remove electrons from conversions via partner track finding, i.e. if there is a general track within $Dist < 0.02$ cm and $\Delta \cot\theta < 0.02$ [**?**]. The impact parameter of the electron track with respect to the position of the primary DA vertex position is required to be below 400 μm in x-y and smaller than 1 cm in z. The cuts are summarised in Table 4.

Table 4: Overview of the electron selection.

Name	Pat memberfunction	Cut
p_T $\|\eta\|$	pt() abs(eta())	$\geq 5.$ ≤ 2.4
Identification	WP95	
Lost hits Partner track finding	gsfTrack–>trackerExpectedHitsInner().numberOfHits() !($\|Dist\|and\|\Delta\cot\theta\|$)	≤ 1 ¡ 0.02
Impact parameter Impact parameter	abs(dxy(pv)) abs(dz(pv))	≤ 0.04 ≤ 1
Isolation Barrel Isolation Barrel	(dr03HcalTowerSumEt + max(0., dr03EcalRecHitSumEt-1.) + dr03TkSumPt) / pt (dr03HcalTowerSumEt + dr03EcalRecHitSumEt + dr03TkSumPt) / pt	≤ 0.15 ≤ 0.15

4.7 Light lepton isolation

A combined relative lepton isolation has been used. The isolation uses information from both calorimeters and the silicon tracker. The isolation value (Iso) is given by the ratio of the sum of all p_T objects within a cone in η-ϕ-space of $\Delta R = \sqrt{\Delta\eta^2 + \Delta\phi^2} < 0.4$ around the lepton and the lepton p_T. It has been pre-calculated in PAT using

$$Iso = \frac{\left[\sum\limits_{photons} p_T + \sum\limits_{neutral\ hadrons} p_T + \sum\limits_{charged\ hadrons} p_T\right]_{dR<0.4}}{p_T} \tag{2}$$

where the first sum runs over the transverse momentum of all particle flow photons, the second sum runs over the transverse momentum of all neutral hadrons and the third sum runs over the transverse momentum deposited as charged hadrons within the cone.

The isolation for prompt muons obtained from the sPlot technique (Sec.**??**) is shown Figure **??** and the cut value is chosen to be $Iso < 0.2$. The distribution for electrons is displayed in Figure **??** and the cut is placed at $Iso < 0.2$ to obtain a similar rejection and efficiency for electrons and muons. The background shapes evaluated from data are discussed in Sec. **??**.

4.8 Taus

TODO: Matthias tau selection

4.9 Jets and missing transverse energy

The anti-kt jet algorithm [6] with a cone size of 0.5 in ΔR is used. Jets are clustered from all reconstructed particle flow particles. We remove jets that are within $\Delta R < 0.4$ to a lepton passing our full lepton selection. Thus we obtain fully lepton cleaned jets in our final selection. The jets are corrected up to level 3 using MC jet energy corrections [17] from the Summer11 (GlobalTag: GR_R_42_V12, START42_V12) production. To correct for PileUp the L1FastJet subtraction using the latest JetMET prescription is applied.

Each corrected jet is required to have a p_T above 30 GeV and the jet axis has to be within $|\eta| < 3$. This relatively tight η cut is used to be able to include tracker information in the jet identification for a large part of the η acceptance and not to rely on the hadronic calorimeter only. Thus, one is able to fully profit from the particle flow algorithm. Each jet has to pass the "FIRSTDATA" "LOOSE" Particle Flow Jet ID criteria, which are used to suppress fake, noise, and badly reconstructed jets, while still retaining as much real jets as possible [18].

The missing transverse energy (MET) is based on the sum of all particle momenta reconstructed using the particle flow event reconstruction (pfMET).

4.10 Trigger

We collect events using three different trigger streams:

- (20,10) GeV ee, $e\mu$, $\mu\mu$ events are selected using the lepton trigger selection.
- (10,10), (10,5), (5,5) GeV ee, $e\mu$, $\mu\mu$ events are selected using the lepton H_T cross object trigger selection.
- (5,15), (10,15), (15,15) GeV $\mu\tau$, $e\tau$, $\tau\tau$ events are selected using the tau trigger selection.

4.10.1 Lepton trigger selection

To collect events for the (20,10) GeV di-lepton selection we use an OR of the following double lepton high level trigger (HLT) paths

- HLT_Ele17_CaloIdL_CaloIsoVL_Ele8_CaloIdL_CaloIsoVL_v*
- HLT_Ele17_CaloIdT_TrkIdVL_CaloIsoVL_TrkIsoVL_Ele8_CaloIdT_TrkIdVL_CaloIsoVL_TrkIsoVL_v*
- HLT_Mu8_Ele17_CaloIdL_v*
- HLT_Mu17_Ele8_CaloIdL_v*
- HLT_Mu10_Ele10_CaloIdL_v*
- HLT_DoubleMu6*
- HLT_DoubleMu7_v*
- HLT_Mu13_Mu7_v*

We check that the prescale of each trigger is set to one for all run ranges.

We measure the eficiency in an orthogonal event selection using events triggered by purely hadronic triggers.

The measured efficiencies are listed in Table 5. We obtain an efficiency of $(99.7 \pm 0.1)\%$, ($(99.7 \pm 0.1)\%$, $(99.7 \pm 0.1)\%$) for the ee ($e\mu$, $\mu\mu$) trigger with respect to the final di-lepton selection, respectively.

Table 5: Double lepton high level trigger efficiencies.

HLT path	Thresh. [GeV]	Pathname	ϵ
H_T	100	HLT_HT100U	$99.8 \pm 0.1\%$
H_T	140	HLT_HT140U	$99.7 \pm 0.1\%$
H_T	150	HLT_HT150U	$99.7 \pm 0.1\%$

4.10.2 Lepton H_T cross trigger trigger selection

To collect events for low lepton p_T range (e 10, μ 5) GeV di-lepton plus H_T cross-object triggers are used. We use an OR of the following double lepton H_T HLT paths

- HLT_DoubleEle8_CaloIdL_TrkIdVL_HT160_v*
- HLT_DoubleEle8_CaloIdL_TrkIdVL_HT150_v*
- HLT_DoubleMu3_HT160_v*
- HLT_DoubleMu3_HT150_v*
- HLT_Mu3_Ele8_CaloIdL_TrkIdVL_HT160_v*
- HLT_Mu3_Ele8_CaloIdL_TrkIdVL_HT150_v*

We check that the prescale of each trigger is set to one for all run ranges.

We measure the leptonic eficiency in event selection using events triggered by purely hadronic (H_T) triggers, while the hadronic efficiency is measured using events collected by di-lepton triggers. We assume no correlation between the hadronic and leptonic part of the trigger and give the total efficiency as a product of both.

Table 6: Double lepton H_T cross object trigger high level trigger efficiencies.

HLT path	Thresh. [GeV]	Pathname	ϵ
H_T	100	HLT_HT100U	$99.8 \pm 0.1\%$
H_T	140	HLT_HT140U	$99.7 \pm 0.1\%$
H_T	150	HLT_HT150U	$99.7 \pm 0.1\%$

The measured efficiencies are listed in Table 6. We obtain an efficiency of $(99.7 \pm 0.1)\%$, $((99.7 \pm 0.1)\%$, $(99.7 \pm 0.1)\%)$ for the ee ($e\mu$, $\mu\mu$) trigger with respect to the final di-lepton selection, respectively.

4.10.3 Tau trigger selection

To collect event including taus in the final state we use an OR of the following double lepton high level trigger (HLT) paths

- **TODO**tau trigger selection

We check that the prescale of each trigger is set to one for all run ranges.

We measure the eficiency in an orthogonal event selection using events triggered by purely hadronic triggers.

Table 7: Tau high level trigger efficiencies.

HLT path	Thresh. [GeV]	Pathname	ϵ
H_T	100	HLT_HT100U	$99.8 \pm 0.1\%$
H_T	140	HLT_HT140U	$99.7 \pm 0.1\%$
H_T	150	HLT_HT150U	$99.7 \pm 0.1\%$

The measured efficiencies are listed in Table 7. We obtain an efficiency of $(99.7 \pm 0.1)\%$, $((99.7 \pm 0.1)\%$, $(99.7 \pm 0.1)\%)$ for the ee ($e\mu$, $\mu\mu$) trigger with respect to the final di-lepton selection, respectively.

5 Efficiency for electrons and muons

The efficiency ratio is derived directly from the data but selection of an inclusive Z boson sample. For this we select di-lepton events (ee, $\mu\mu$) with (20,10) GeV including the lepton trigger paths listed in Sec.??.

We apply an cut in the invariant mass of $60 < m_{ll} < 120$ GeV to obtain a pure Z boson sample. The differnt flavour subtraction described in Sec. 7.1 relies on the knowledge of the electron to muon efficiency ratio, which we derive from this sample as

$$r_{\mu e} = \sqrt{\frac{n_{\mu\mu}}{n_{ee}}} = 1.13 \pm 0.07 \tag{3}$$

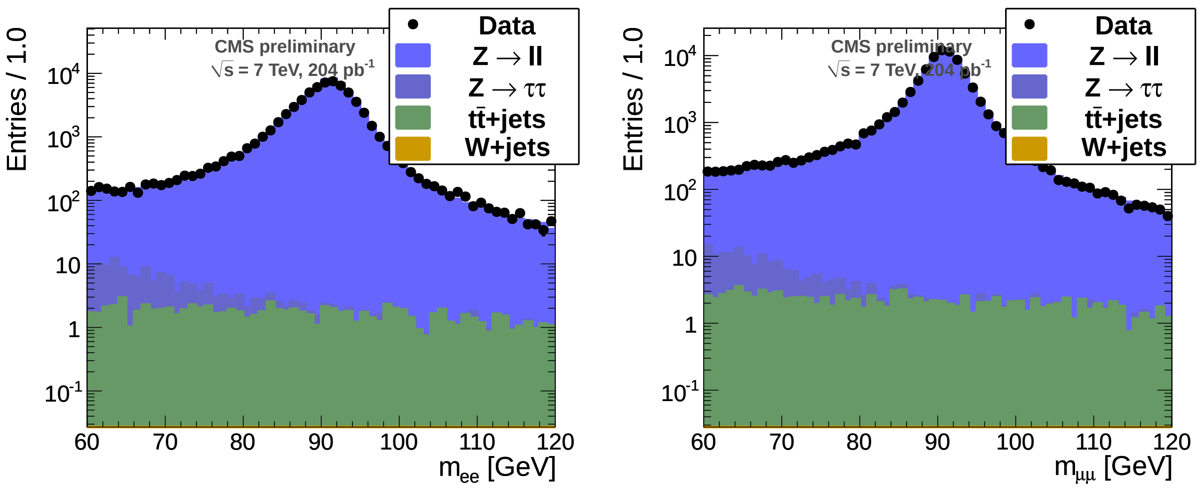

(a) (b)

Figure 1: Invariant mass distributions for a (20,10) GeV di-lepton selection after leptonic trigger requirement.

Table 8: Muon to electron reconstruction efficiency ratio obtained from a Z boson selection on data and $Z+$jets Monte Carlo simulation.

	Data	Monte Carlo
ratio $r_{\mu e}$	1.07 ± 0.005(stat) ± 0.05(syst)	1.052 ± 0.003(stat)

Since we measure the efficiency on a Z sample, which has a different jet multiplicity compared to a ttbar sample, we need to assign a systematic uncertainty in the extrapolation. We test the dependence in simulation by comparing a top MC sample with Z-boson simulation. While the absolute efficiency drops, the ratio of the electron to muon efficiency is approximately constant (within 5%), meaning that the loss in efficiency is the same for both lepton flavours. We therefore assume 5% additional systematic uncertainty on the ratio.

6 Event selection

For all event selections presented later on the main backgrounds are

Top pairs Top pair events are the dominant SM background to the search, since they contain real opposite sign leptons, missing transverse energy and a non negligible jet activity. This background is estimated by the opposite flavour subtraction.

Z+jets Events with a Z Boson contain two opposite sign leptons and can contain a high jet activity, but the missing transverse energy is always instrumental and therefore the background can be reduced completely. This backround can be estimated using the JZB method [22] and is found to be very small in the signal region.

W+jets Events with a W Boson contain real missing transverse energy and can contain a high jet activity, but do only contain one lepton. Therefore the background can be measured using the fake lepton component. This background is estimated by the isolation template method.

Diboson Events with two gauge bosons do contribute to the background. Due to the low cross-section of the process their contribution is found to be negligible. This background is estimated from MC.

QCD Although the di-jet cross-section is huge, this background is found to be negligible in MC, since all cuts act very well on QCD (no isolated leptons, no missing transverse energy and a steeply falling H_T distribution). This background is estimated by the isolation template method.

6.1 Preselection

For now we select only events using the lepton trigger selection, but lower $p_\perp$ leptons can be added without any changes to the presented methods. We start from a common preselection defined as

- Two leptons of opposite sign with the thresholds of $p_T > 20$ GeV for the hardest and $p_T > 10$ GeV for the second lepton.
- At least two jets and a $H_T > 100$ GeV.
- A missing transverse energy of at least $\not\!\!E_T > 100$ GeV.

The region is expected to be dominated by events with di-leptonic top decays. The yields in data and simulation are given in Tab. 9

Table 9: Summary of number of events expected from Monte Carlo simulations in the signal region of $H_T >$ 100 GeV and $\not\!\!E_T > 100$ GeV. The errors reflect the Monte Carlo statistics only.

Process	ee	$\mu\mu$	$e\mu$	total
$t\bar{t}$	0.39 ± 0.04	0.5 ± 0.05	0.79 ± 0.06	1.68 ± 0.09
$Z+$jets	0.0 ± 0.07	0.08 ± 0.05	0.11 ± 0.07	0.19 ± 0.11
$W+$jets	0.0 ± 0.32	0.0 ± 0.32	0.0 ± 0.32	0.0 ± 0.32
Di-boson	0.02 ± 0.01	0.03 ± 0.01	0.03 ± 0.01	0.08 ± 0.02
Total background	0.41 ± 0.33	0.53 ± 0.33	$1. \pm 0.33$	$2. \pm 0.32$
Data	0	0	1	1
LM0	3.41 ± 0.17	3.91 ± 0.17	4.52 ± 0.14	11.84 ± 0.42
LM1	1.64 ± 0.04	2.02 ± 0.04	1.01 ± 0.03	4.64 ± 0.07

6.2 Definition of the signal regions

To be prepared for a much larger luminosity we define tighter signal regions for an intgrated luminosity of up to 1 fb^{-1}.

6.2.1 2010 signal region

For reference we keep the signal region used in 2010. It is defined by tightening both H_T and $\not\!\!E_T$ from the preselection region

- A $H_T > 350$ GeV.
- A $\not\!\!E_T > 150$ GeV.

The $\not\!\!E_T$ distribution after application of the H_T cut is shown in Fig 2(a) and the yield split by flavour for a cut at 150 GeV is listed in Tab. 10.

6.2.2 High H_T signal region

A signal region with high H_T is defined by tightening the H_T from the preselection region

- A $H_T > 600$ GeV.

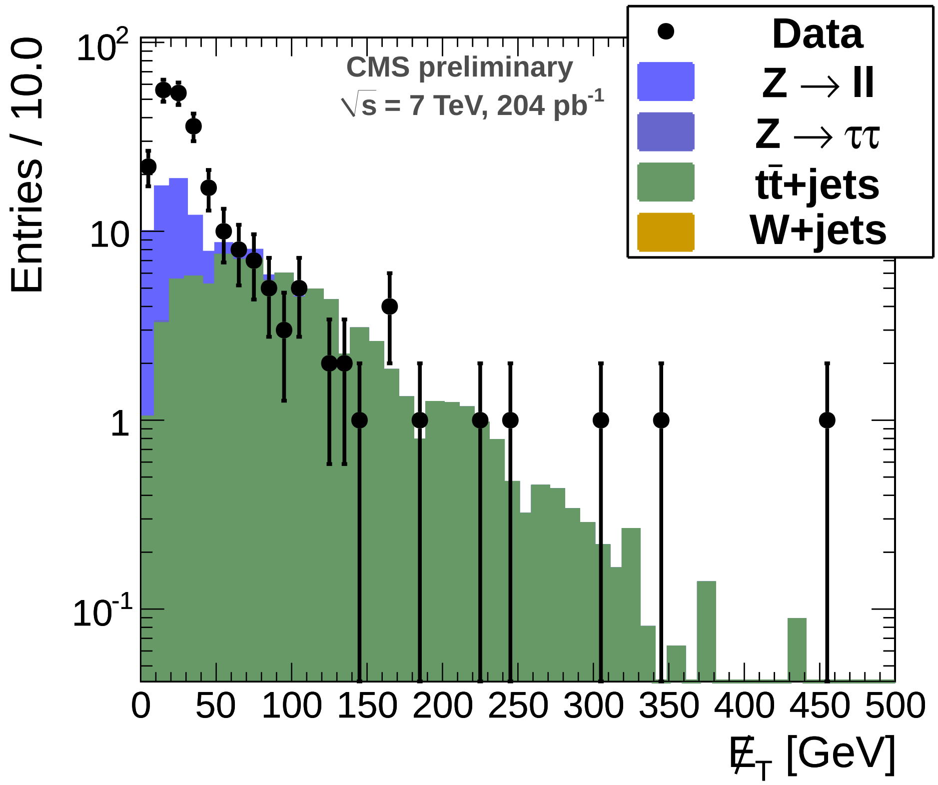

(a)

Figure 2: $\not\!\!E_T$ distribution for all events passing di-lepton selection and satisy $H_T > 350$ GeV. For the final $\not\!\!E_T$ selection (150) GeV the selection is dominated by $t\bar{t}$.

Table 10: Summary of number of events expected from Monte Carlo simulations in the signal region of $H_T >$ 350 GeV and $\not\!\!E_T > 150$ GeV. The errors reflect the Monte Carlo (scaled to 204 pb^{-1}) statistics only.

Process	ee	$\mu\mu$	$e\mu$	total
$t\bar{t}$	0.39 ± 0.04	0.5 ± 0.05	0.79 ± 0.06	1.68 ± 0.09
$Z +$ jets	0.0 ± 0.07	0.08 ± 0.05	0.11 ± 0.07	0.19 ± 0.11
$W +$ jets	0.0 ± 0.32	0.0 ± 0.32	0.0 ± 0.32	0.0 ± 0.32
Di-boson	0.02 ± 0.01	0.03 ± 0.01	0.03 ± 0.01	0.08 ± 0.02
Total background	0.41 ± 0.33	0.53 ± 0.33	$1. \pm 0.33$	$2. \pm 0.32$
Data	0	0	1	1
LM0	3.41 ± 0.17	3.91 ± 0.17	4.52 ± 0.14	11.84 ± 0.42
LM1	1.64 ± 0.04	2.02 ± 0.04	1.01 ± 0.03	4.64 ± 0.07

- A $\not\!\!E_T > 100$ GeV.

The $\not\!\!E_T$ distribution after application of the H_T cut is shown in Fig 4(a) and the yield split by flavour for a cut at 150 GeV is listed in Tab. 11.

6.2.3 High $\not\!\!E_T$ signal region

A signal region with high $\not\!\!E_T$ is defined by slightly tightening the H_T and a much tighter $\not\!\!E_T$ selection compared to the pre-selection region

- A $H_T > 250$ GeV.
- A $\not\!\!E_T > 250$ GeV.

The $\not\!\!E_T$ distribution after application of the H_T cut is shown in Fig 4(a) and the yield split by flavour for a cut at 250 GeV is listed in Tab. 12.

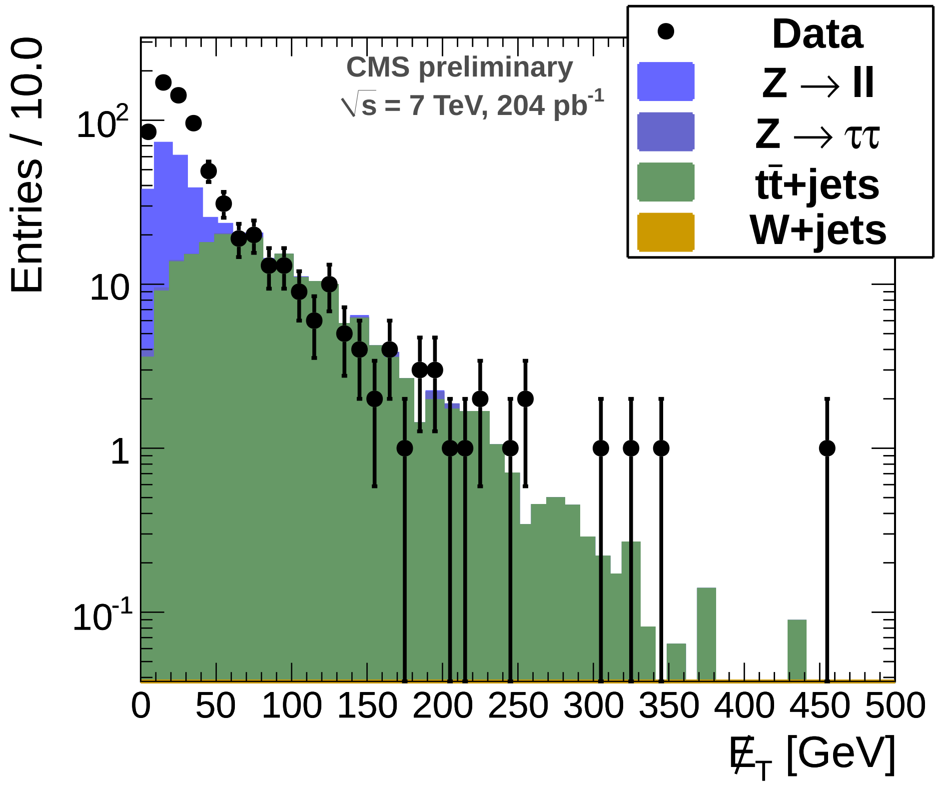

(a)

Figure 3: $\not{E}_T$ distribution for all events passing di-lepton selection and satisfy $H_T > 600$ GeV. For the final $\not{E}_T$ selection (100) GeV the selection is dominated by $t\bar{t}$.

Table 11: Summary of number of events expected from Monte Carlo simulations in the signal region of $H_T > 600$ GeV and $\not{E}_T > 100$ GeV. The errors reflect the Monte Carlo (scaled to 204 pb^{-1}) statistics only.

Process	ee	$\mu\mu$	$e\mu$	total
$t\bar{t}$	0.39 ± 0.04	0.5 ± 0.05	0.79 ± 0.06	1.68 ± 0.09
$Z+$jets	0.0 ± 0.07	0.08 ± 0.05	0.11 ± 0.07	0.19 ± 0.11
$W+$jets	0.0 ± 0.32	0.0 ± 0.32	0.0 ± 0.32	0.0 ± 0.32
Di-boson	0.02 ± 0.01	0.03 ± 0.01	0.03 ± 0.01	0.08 ± 0.02
Total background	0.41 ± 0.33	0.53 ± 0.33	$1. \pm 0.33$	$2. \pm 0.32$
Data	0	0	1	1
LM0	3.41 ± 0.17	3.91 ± 0.17	4.52 ± 0.14	11.84 ± 0.42
LM1	1.64 ± 0.04	2.02 ± 0.04	1.01 ± 0.03	4.64 ± 0.07

7 Background prediction methos

7.1 Different flavour subtraction

Since the signal region is expected to be absolutely dominated by $t\bar{t}$-production we use the opposite flavour subtraction to predict backgrounds where uncorrelated leptons are being produced. It relies only on the knowledge of the ratio of electron to muon reconstruction efficiency $r_{e\mu}$, which we derive in Sec. 5.

Under the assumption of lepton unversality The following two formulas hold for any background where di-leptons are being produced uncorrelated (e.g. top-pairs events, $Z \rightarrow \tau^+\tau- \rightarrow l^+l^-$, WW-production):

$$n_{ee} = \frac{1}{2} n_{e\mu} r_{\mu e}, \quad n_{\mu\mu} = \frac{1}{2} \frac{n_{e\mu}}{r_{\mu e}}.$$

A closure test of the method has been performed using a simulated top-pair sample and we observe a good agreement between prediction and MC truth:

$$n_{ee} = 16.9 \pm 2.8(\text{stat.}) \;\; (16.2 \text{ MC}), \quad n_{\mu\mu} = 19.8 \pm 3.3(\text{stat.}) \;\; (21.5 \text{ MC}).$$

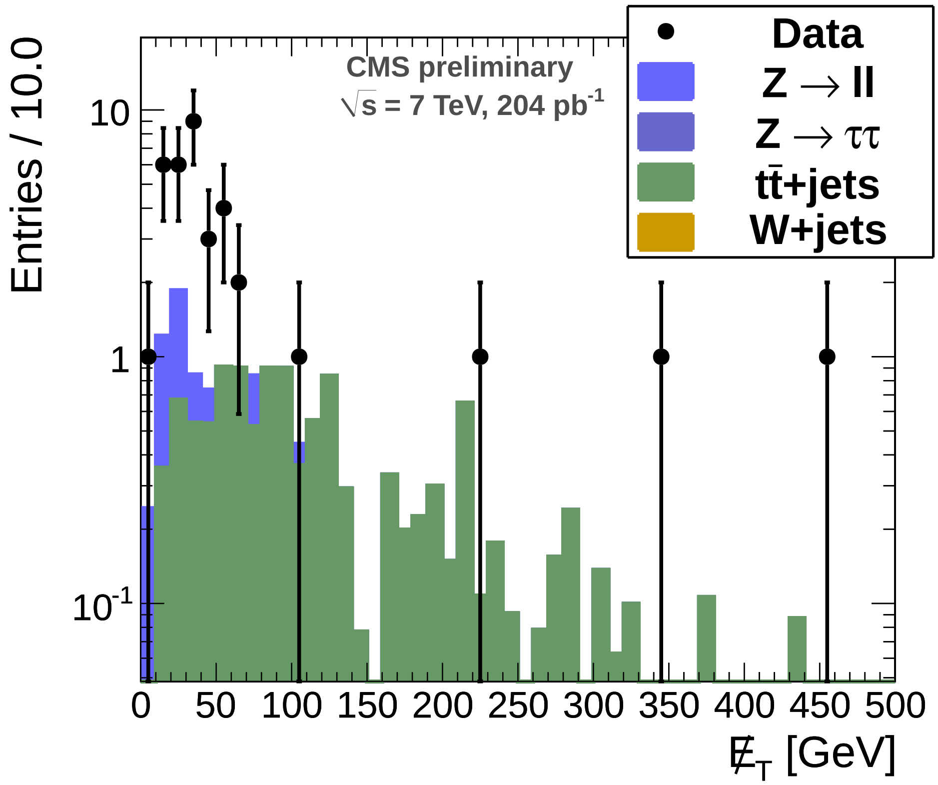

(a)

Figure 4: $\not\!\!E_T$ distribution for all events passing di-lepton selection and satisfy $H_T > 250$ GeV. For the final $\not\!\!E_T$ selection (250) GeV the selection is dominated by $t\bar{t}$.

Table 12: Summary of number of events expected from Monte Carlo simulations in the signal region of $H_T >$ 250 GeV and $\not\!\!E_T > 250$ GeV. The errors reflect the Monte Carlo (scaled to 204 pb^{-1}) statistics only.

Process	ee	$\mu\mu$	$e\mu$	total
$t\bar{t}$	0.39 ± 0.04	0.5 ± 0.05	0.79 ± 0.06	1.68 ± 0.09
$Z +$ jets	0.0 ± 0.07	0.08 ± 0.05	0.11 ± 0.07	0.19 ± 0.11
$W +$ jets	0.0 ± 0.32	0.0 ± 0.32	0.0 ± 0.32	0.0 ± 0.32
Di-boson	0.02 ± 0.01	0.03 ± 0.01	0.03 ± 0.01	0.08 ± 0.02
Total background	0.41 ± 0.33	0.53 ± 0.33	$1. \pm 0.33$	$2. \pm 0.32$
Data	0	0	1	1
LM0	3.41 ± 0.17	3.91 ± 0.17	4.52 ± 0.14	11.84 ± 0.42
LM1	1.64 ± 0.04	2.02 ± 0.04	1.01 ± 0.03	4.64 ± 0.07

7.2 Control Region

To gain confidence in the performance of this technique we wish to test it on a high statistic sample, dominated by $t\bar{t}$, as is our expected signal region is. To do this, we are required to use the leptonic trigger sample, described in [24] including the lepton p_T thresholds of 20 (10) GeV, since we need to lower the H_T requirement inherent in the hadronic trigger sample. Using this sample our control region is defined by: $100 < H_T < 350$ GeV and $\not\!\!E_T > 80$ GeV, where we expect almost no Z+Jets contribution anymore and are dominated by $t\bar{t}$. The control region is disjunct from the signal region, however it also suffers, from potential signal contamination, in case of a very soft $\not\!\!E_T$ spectrum of the new physics. The distribution of the events in the invariant mass distribution split by lepton flavour combinations is shown in Fig. **??**.

In this region we observe 26 opposite flavour opposite sign candidates and subtract 1.0 ± 0.5 predicted fake events. Therefore we obtain 25.0 ± 0.5 $t\bar{t}$- like candidate events, which we use to obtain a prediction for the same flavour combinations using the ratio of Tab. .

Table 13 shows the number of expected SM background events in the control region $100 < H_T < 350$ GeV and

$\not\!\!E_T > 80$ GeV, as well as the prediction from the background estimation techniques, for an integrated luminosity of 35 pb^{-1}. We observe a good agreement between prediction and observation.

Table 13: Number of predicted and observed events in the control region, defined as: $100 < H_T < 350$ GeV and $\vec{\not\!\!E}_T > 80$ GeV.

	Control Region	
Process	ee	$\mu\mu$
$t\bar{t}$ from $e\mu$	11.7 ± 2.4	13.4 ± 2.8
Fake leptons	0.5 ± 0.3	0.4 ± 0.2
Total predicted	12.2 ± 2.4	13.8 ± 2.8
Total observed	10	15
SM MC	8.4 ± 0.2	10.5 ± 0.3
LM0	3.7 ± 0.2	4.2 ± 0.2
LM1	0.5 ± 0.1	0.7 ± 0.1

8 Results

The SM background predictions in the signal region are summarized in Tab. 14. Some control distributions after the opposite sign dilepton selection and H_T requirement are shown in Appendix **??**. We observe a good data to MC agreement and do not observe a large number of fake leptons even without $\not\!\!E_T$ requirement. In the signal region we observe one event in the $e\mu$-category and an event display is in Appendix **??**.

Additionally the consistency of the background prediction method is checked in the control region, where we predict 25.0 ± 5.0 same-flavor events and observe 25 (Sec. 7.1).

Table 14: Number of predicted and observed events in the signal region, defined as: $H_T > 350$ GeV and $\vec{\not\!\!E}_T > 150$.

	Signal Region	
Process	ee	$\mu\mu$
$t\bar{t}$ from $e\mu$	$0.4^{+1.0}_{-0.4}$	$0.5^{+1.2}_{-0.4}$
Fake leptons	0	0
Total predicted	$0.4^{+1.0}_{-0.4}$	$0.5^{+1.2}_{-0.4}$
Total observed	0	0
SM MC	0.38 ± 0.08	0.56 ± 0.07
LM0	3.4 ± 0.2	3.9 ± 0.2
LM1	1.6 ± 0.1	2.0 ± 0.1

We find one event in the signal region in the $e\mu$-lepton combination with a fake prediction of 0.1 ± 0.1, and thus predict $0.9^{+2.2}_{-0.8}$ same-flavour events. In data we find no same-flavour events and have to contrast this with 7.3 ± 1.6 and (3.6 ± 0.7) expected events at the benchmark points LM0 (LM1).

9 Systematic uncertainties

Systematic uncerteinties arise from uncertainties of the event selection expected in simulation compared to the performance from the actual detector. A global normalisation uncertainty comes from an uncertainty on the total integrated luminosity of 11% [28].

9.1 Systematic uncertainty for the lepton selection

We do observe a good agreement from tag and probe within 2%. In simulation the difference of the lepton selection between Z+jets and top-pair events is within 7%, which we use as a systematic uncertainty. The inclusive lepton efficiency of leptons in the mSUGRA benchmark points differ by 25% to the efficiency measured at the Z resonace. However this drop in efficiency is simulated by the MC. We take 10% uncertainty on the leptonic part as a systematic uncertainty in the limit setting procedure.

9.2 Pile-up

Since the lepton efficiency is measured including pile-up, we include the effect and do not correct for the difference in lepton selection efficiency. Nevertheless pile-up has some effect on the jet and missing transvers energy selection. It has been studied in simulation and found to be negligible for the high H_T and $\not\!\!E_T$ selection. Therefore no additional uncertainty is assigned to account for pile-up. For leptons above 10 GeV the effect of pile-up in the isolation is below 3% per lepton and therefore we do not assign an additional systematic uncertainty.

9.3 Uncertainty on the hadronic selection

The uncertainty on the jet-energy-scale is smaller than 5% for particle flow jets [29]. This uncertainty directly translates into a scale uncertainty on the H_T selection. For particle flow MET and uncertainty on the scale of 5% is assumed [30]. We vary both fully correlated and find that it changes the acceptance at LM0 by 12%, while the change at LM1 is smaller (5%). We take this as systematic uncertainty in the limit setting method. The uncertainty in the $t\bar{t}$-sample is found to be 30% in the final signal selection, while it is smaller in the leptonic control region (7%). This enters the predicted number from simulation.

9.4 Uncertainty on the fake background prediction

For the fake-component of the background a uncertainty of 50% is assumed, which is described in detail in Sec. **??**.

The main uncertainty for the opposite flavour subtraction arises from the uncertainty on the lepton selection in a hadronic event environment. While the inclusive efficiency for leptons originating from the Z-Boson can be determined with a systematic uncertainty of 2%, it cannot be determined with that precision in the kinematic regime of the search. Therefore the difference between the efficiency from the Z and $t\bar{t}$ is assumed as a systematic uncertainty (5%).

The systematic uncertainties on the yields from simulation are summarised in Tab. 15.

Table 15: Summary of the systematic uncertainties for

Systematic uncertainty	$t\bar{t}$	LM0	LM1
Cross-section	39%	-	-
H_T + $\not\!\!E_T$	30%	12%	5%
Lepton	10%	15%	15%
Luminosity	11%	11%	11%
Total	51%	22%	19%

10 Limit

As discussed in Section 8, we see no event in the signal region, defined as H_T >350 GeV and $\not\!\!E_T > 150$ GeV and two same flavour opposite sign leptons.

The background prediction from the SM Monte Carlo is 0.77 $\pm$ 0.26 events, where the uncertainty comes from the jet energy scale (30%, see Section 9), the luminosity (11%), and the lepton/trigger efficiency (10%)[2)]. The opposite flavor based background prediction is $0.9^{+2.2}_{-0.8}$.

The background prediction is well in agreement with the prediction from simulation and with the observation of no events.

We calculate a Bayesian 95% CL upper limit [26] on the number of non SM events in this signal region to be 3.0.

We cross-checked the code with a Bayesian 95% CL upper limit using the MCMC calculator[27] and get the same result of 3.0.

Here as well, we remind the reader of the number of expected LM0 and LM1 events from Table **??**: 7.3 ± 1.6 events and 3.3 ± 0.7 respectively, where the uncertainties are from energy scale (Section 9), luminosity, and lepton efficiency.

2) Other uncertainties associated with the modeling of $t\bar{t}$ in MadGraph have not been evaluated.

We thus can exclude LM0 95% confidence level.

11 Conclusion

We have presented a SUSY search for correlated flavour production in the opposite-sign channel in the presence of high H_T and $\not\!\!E_T$. We observe good agreement between data and simulation as well as to our background prediction method. We conclude that there is no sign of flavour correlated production and set a limit 3.0 signal events at 95% confidence level within acceptance of our selection. This excludes the discussed benchmark points LM0.

12 Acknowledgements

References

[1] B.C. Alanach, *"SOFTSUSY: a program for calculating supersymmetric spectra"*, Comput.Phys.Commun. 143:305-331, 2002

[2] A. Djouadi et al, *Decays of Supersymmetric Particles: the program SUSY-HIT (SUspect-SdecaY-Hdecay-InTerface)* ActaPhys.Polon. B38:635-644, 2007.

[3] T. Sjostrand et al, *"PYTHIA 6.4 Physics and Manual"*, JHEP 0605:026, 2006

[4] W. Beenakker et al, *"Squark and Gluino Production at Hadron Colliders"*, Nucl.Phys. B492:51-103, 1997

[5] The CMS Collaboration, *"Study of the Z production in association with jets in proton-proton collisions at $\sqrt{s} = 10$ TeV with the CMS detector at the CERN LHC"*, CMS Physics Analysis Summary JME-08-006

[6] M. Cacciar et al, *"The anti-k_t jet clustering algorithm"*, JHEP 0804:063, 2008

[7] J. Alwall et al, *"MadGraph/MadEvent v4: The New Web Generation"*, JHEP 0709:028, 2007

[8] M. Cacciari et al, *"Updated predictions for the total production cross sections of top and of heavier quark pairs at the Tevatron and at the LHC"*, JHEP 0809:127, 2008

[9] S. Frixione, M.L. Mangano, *"How accurately can we measure the W cross section?"*, JHEP 0405:056, 2004

[10] M. Pivk and F.R. Le Diberder, *A statistical tool to unfold data distributions*, arXiv:physics/0402083

[11] V+jets wiki, `https://twiki.cern.ch/twiki/bin/view/CMS/VplusJets`

[12] M. Mulders et al. *"Muon Identification in CMS"*, CMS Analysis Note 2008/098

[13] J. Branson et al. *"A cut based method for electron identification in CMS"*, CMS Analysis Note 2008/082

[14] F. Beaudette et al. *"Electron Reconstruction within the Particle Flow Algorithm"*, CMS Analysis Note 2010/034

[15] M. Bachtis et al. *"Commissioning of the Particle-flow Event Reconstruction with the first LHC collisions recorded in the CMS detector"*, CMS Analysis Note 2010/???

[16] G. P. Salam, G. Soyez, *"A practical Seedless Infrared-Safe Cone jet algorithm"*, JHEP 0705:086, 2007

[17] The CMS Collaboration, *"Plans for Jet Energy Corrections at CMS"*, CMS Physics Analysis Summary JME-07-002

[18] N. Saoulidou, *"Particle Flow Jet Identification Criteria"*, CMS Analysis Note 2009/???

[19] W. Verkerke, D. Kirkby, *"The RooFit toolkit for data modeling"*, arXiv:physics/0306116

[20] The CMS Collaboration, *"Performance of muon identification in pp collisions at $\sqrt{s} = 7$ TeV"*, CMS Physics Analysis Summary MUO-10-002

[21] The CMS Collaboration, *"Performance of Methods for Data-Driven Background Estimation in SUSY Searches"*, CMS Physics Analysis Summary SUS-10-001

[22] K. Theofilatos et al. *"SUSY Searches in the $Z^0 + 3$ jets + $\not\!\!E_T$ Final State with Data-driven Background Estimation"*, CMS Analysis Note 2009/132

[23] A. Singh et al. *"SUSY in the $Z/\gamma * +$ Jet(s) + $\not\!\!E_T$ Final State Using Particle Flow"*, CMS Analysis Note 2010/250

[24] B. Hooberman et al. *"Search for new physics in the opposite sign dilepton sample"*, CMS Analysis Note 2010/370

[25] J. Conway, `https://twiki.cern.ch/twiki/bin/view/CMS/PileupInformation`

[26] J. Conway, `http://www-cdf.fnal.gov/physics/statistics/code/bayes.f`

[27] RooStats wiki, `https://twiki.cern.ch/twiki/bin/view/RooStats/WebHome`

[28] The CMS Collaboration, *"Measurement of CMS Luminosity"*, CMS Physics Analysis Summary EWK-10-004

[29] The CMS Collaboration, *"Jet Energy Corrections determination at $\sqrt{s} = 7$ TeV"*, CMS Physics Analysis Summary JME-10-010

[30] The CMS Collaboration, *"MET Performance in Events Containing Electroweak Bosons from pp Collisions at $\sqrt{s} = 7$ TeV"*, CMS Physics Analysis Summary JME-10-005